Engineering *Yarrowia lipolytica* to produce itaconic acid from waste cooking oil

Lanxin Rong[1], Lin Miao[1], Shuhui Wang[1], Yaping Wang[1], Shiqi Liu[1], Zhihui Lu[1], Baixiang Zhao[1], Cuiying Zhang[1], Dongguang Xiao[1], Krithi Pushpanathan[2], Adison Wong[2**], Aiqun Yu[1*]

[1]State Key Laboratory of Food Nutrition and Safety, Key Laboratory of Industrial Fermentation Microbiology of the Ministry of Education, Tianjin Key Laboratory of Industrial Microbiology, College of Biotechnology, Tianjin University of Science and Technology, No.29 the 13th Street TEDA, Tianjin 300457, PR China

[2]Food, Chemical and Biotechnology Cluster, Singapore Institute of Technology, Singapore 138683, Singapore

**Co-corresponding author: Dr. Adison Wong, [Assistant Professor], [Singapore Institute of Technology], E-mail: adison.wong@singaporetech.edu.sg, Tel: +65 65921626

*Corresponding author: Dr. Aiqun Yu, [Professor], [Tianjin University of Science and Technology], E-mail: yuaiqun@tust.edu.cn, Tel: +86 22 60602723

Abstract

Itaconic acid (IA) is a high-value organic acid with a plethora of industrial applications. In this study, we seek to develop a microbial cell factory that could utilize waste cooking oil (WCO) as raw material for circular and cost-effective production of the abovementioned biochemical. Specifically, we expressed cis-aconitic acid decarboxylase (*CAD*) gene from *Aspergillus terreus in* either the cytosol or peroxisome of *Y. lipolytica* and assayed for production of IA on WCO. To further improve production yield, the 10 genes involved in the production pathway of acetyl-CoA, an intermediate metabolite necessary for the synthesis of cis-aconitic acid, were individually overexpressed and investigated for their impact on IA production. To minimize off-target flux channeling, we had also knocked out genes related to competing pathways in the peroxisome. Impressively, IA titer up to 54.55 g/L was achieved in our engineered *Y. lipolytica* in a 5L bioreactor using WCO as the sole carbon source.

Keywords: Itaconic acid, *Y. lipolytica*, Waste cooking oil, Peroxisome, Subcellular engineering

1. Introduction

Carboxylic acids are important building blocks in the chemical industry. Among them, itaconic acid (IA) is favorably listed by the US Department of Energy as one of top 12 biochemical to be produced from renewable resources (Werpy et al., 2004), with a forecasted market potential of $260 million in 2025 (Sriariyanun et al., 2019). IA is an unsaturated dicarboxylic acid that is characteristically stable in acidic, neutral and moderately alkaline conditions. Due to its advantageous properties, IA is often used as a co-monomer in the manufacture of synthetic fibers, coatings, adhesives, thickeners

and binders (Zhao et al., 2018; Willke et al., 2001), and as substitutes for petrochemical-based acrylic or methacrylic acids (Nuss et al., 2013). Traditionally, to meet the growing demand for IA, industries resort to fossil resources through petrochemical refinery processes to produce IA at scale. However, these methods often suffer from low efficiency and generate large amount of waste in the process, such as spent heavy metal catalysts and organic solvents (Krull et al., 2017). Furthermore, fossil resources are finite and will eventually be depleted. For these reasons, bio-based production of IA using microbial cell factories are increasingly being pursued.

Filamentous fungi such as *Aspergillus terreus* (Kuenz et al., 2012), *Ustilago maydis* (Geiser et al., 2016) and *Ustilago cynodontis* (Tehrani et al., 2019b) have been demonstrated to naturally produce IA at high titers. In one example, the fermentation of *A. terreus* at industrial scale is able to generate a titer of 160 g/L IA (Krull et al., 2017), a value that is close to the theoretical yield. In another example, up to 220g/L IA was achieved by fermentation of *U. maydis* (Tehrani et al., 2019a). Despite having high production titers, current bioprocesses involving filamentous fungi are not without challenges. Critically, the highly branched mycelial filaments of filamentous fungi give rise to high broth viscosity during fermentation, leading to poor aeration and mixing in stirred-tank bioreactors (Porro et al., 2017; Kubicek et al., 2011). Increasing impeller speed, on the other hand, is not an option due to the shear-sensitive nature of filamentous fungi. Moreover, fermentation of most filamentous fungi requires the addition of alkali to maintain a neutral pH condition which is a cause of concern as this increases the probability of bacterial contamination during cultivation (Cui et al., 2017). To circumvent issues associated with filamentous fungi bioprocessing, scientists have applied systems metabolic engineering principles to enable heterologous production of

IA in several strains of bacteria and yeasts (Table 1).

The industrial microbe *Yarrowia lipolytica* is an unconventional oleaginous yeast that is also classified by the US Food and Drug Administration as 'generally regarded as safe' (GRAS) (Zhao et al., 2021b). *Y. lipolytica* possesses unique physiological and metabolic features that enhance its merits as a microbial cell factory. Firstly, *Yarrowia* has good tolerance for external environment stresses, such as low temperatures, high salt concentrations and acidic pH (Gonçalves et al., 2014). Secondly, the oleaginous yeast is able to utilize a myriad of carbon substrates for growth, including waste cooking oil (WCO) (Li et al., 2022; Zinjarde, 2014; Pang et al., 2019). This permits the valorization of waste streams and reduces the overall cost of production. Thirdly, *Yarrowia* is richly endowed with multiple pathways for the generation and accumulation of intracellular acetyl-CoA, which are important intermediaries of IA biosynthesis (Ng et al., 2020; Zhou et al., 2012). Finally, the yeast exhibits high tolerance for IA, thus allowing for accumulation of IA within (Zhao et al., 2019).

In our previous studies, we successfully engineered *Y. lipolytica* to produce limonene and bisabolene, where WCO was employed as the sole carbon source (Pang et al., 2019; Li et al., 2022; Zhao et al., 2021b). Motivated by earlier successes, we herein investigated the feasibility of producing IA from engineered *Y. lipolytica* on waste cooking oil. We expressed cis-aconitic acid decarboxylase (*CAD*) gene from *A. terreus in* either the cytosol or peroxisome of *Y. lipolytica* and assayed for production of IA in the extracellular supernatant. To further improve the final yield, the 10 genes involved in the production pathway of acetyl-CoA, an intermediate metabolite necessary for the synthesis of cis-aconitic acid, were each singly overexpressed. To minimize off-target flux channeling, we had also knocked out genes related to competing pathways in the

peroxisome. Finally, IA titer up to 54.55 g/L was obtained in the engineered *Y. lipolytica* with a yield of 0.3 g/g WCO and a maximum productivity of 0.6 g/L/h without pH control in the 5-L bioreactor. At the time of writing, this is the highest titer of IA obtained with an engineered yeast cell factory.

2. Materials and methods

2.1. Strains, plasmids, primers, and cultivation media

The *Escherichia coli* strain DH5α was used as the host in this study for the cloning and plasmid construction. *E. coli* strains were routinely cultured at 37 °C in Luria−Bertani (LB) media (1% tryptone, 0.5% yeast extract, and 1% sodium chloride contained) or on LB agar plates supplemented with 100 μg/mL of ampicillin. *Y. lipolytica* Po1g KU70Δ was used as the base strain in this study, which has been generated from the parental strain Po1g (a commonly used host strain for protein expression). This strain was used as it is known that the rate of precise homologous recombination (HR) increased substantially for deletion of the *KU70* gene in Po1g (Yu et al., 2016). Routine cultivation of *Y. lipolytica* strains was carried out at 30 °C in YPD medium (1% yeast extract, 2% peptone and 2% dextrose contained) while the yeast synthetic complete medium (YNB) (0.67% yeast nitrogen base without amino acids, 2% glucose, 1.5% Bacto agar) lacking the appropriate nutrients was used for the screening of transformants. The fermentation experiment used YPO medium containing WCO (1% yeast extract, 2% peptone, 1.18% WCO and 0.2% tween-80 contained), and the initial pH of cultivation media was 5.73. Among them, the amount of WCO added is calculated based on the same C atoms as glucose in YPD medium. The strains and plasmids used in this study were listed in Table S1. The PCR primers used in this study were synthesized by Genewiz (Jiangsu, China) and were listed in Table S2.

2.2. Plasmid construction

The *Y. lipolytica* expression vector pYLEX1 used in this study possesses the strong promoter hp4d, and its detailed information was provided in Li et al., 2021. Using primers CAD1-F/R and CAD2-F/R that were synthesized according to the existing sequences (GenBank ID: AB326105.1) in NCBI GenBank, two fragments of the *CAD* gene without introns were amplified from the *A. terreus* HAT418 genome and cloned into pYLEX1 to yield pYLEX1-CAD through adapted homologous recombination. The construction process of plasmid pYLEX1-CAD is depicted in Figure S1. The sequences of the oligonucleotides used to amplify all the genes are listed in Table S2 in the Additional File. Subsequently, the expression cassettes of other gene candidates were cloned into pYLEX1-CAD individually (Figure S2). All recombinant plasmids were constructed using the One Step Cloning Kit from Vazyme Biotech Co., Ltd. (Nanjing, China). Transformants were plated on LB-ampicillin agar plates and incubated overnight at 37 °C. Single colonies were inoculated into LB-ampicillin and cultured overnight at 37 °C with shaking at 225 rpm. Plasmids were isolated, and the genes were verified by DNA sequencing.

Following that, all plasmids were linearized using the *Spe* I enzyme and then transformed into the *Y. lipolytica* Po1g KU70Δ competent cells using lithium acetate/single-stranded vector DNA/polyethylene glycol method. The linearized plasmids introduced were integrated at the pBR322 locus of the strain Po1g KU70Δ. After two to three days of culture, the positive *Y. lipolytica* KU70Δ transformants were selected on YNB-LEU plates and subsequently confirmed by genomic DNA PCR analysis (Yu et al., 2016). Accordingly, in this study, the engineered *Y. lipolytica* Po1g KU70Δ strain was used as the host for all genetic modifications with gene knockouts

and chromosomal expression constructs introduced via engineered pYLEX1 plasmids.

2.3. Yeast cultivation

Seed inoculum of *Y. lipolytica* were first cultured in a 20 mL tube with 5 mL YPD medium and incubated for 24 h in a shaking incubator set at 30 ℃ and 220 rpm. Next, a 250 mL flask was filled with 50 mL YPO medium and inoculated at the seeding density of OD_{600} 0.1. The inoculated finished shake flasks were grown in a shaking incubator set at 30 °C and 220 rpm. Fermented yeast cultures were collected on the fourth day and analyzed by GC-MS to determine and identify the IA content.

2.4. Gene Knockout

The *ICL*Δ strain was generated by knocking out the ORF region gene of *ICL* via the homologous recombination (HR) mechanism with the cassette of the hygromycin B resistance marker gene (*HPH)* amplified from pSH69-Hph using the primer pairs ICL-Hph-F/R. To this end, two targeting arms (upstream and downstream flanking sequences of *ICL*), each approximately 1000 bp in length, were amplified using PCR from the genomic DNA of Po1g-2G and ligated to the 5' and 3' ends of the *HPH* gene, respectively. After transformation of the *ICL* disruption cassette into *Y. lipolytica* cells, a gene replacement event occurs via double-crossover homologous recombination within the two flanking homology arms at the targeted locus. Transformants were grown in the YPDH solid medium (30 ℃, under dark conditions) supplemented with hygromycin and chosen randomly. The correct *ICL*Δ strain was confirmed by PCR with ICL-Hph-knock-F and ICL-Hph-knock-R primers. The construction of the *CAT*Δ strain was carried out using a similar procedure.

2.5. Visualizing fluorescence distribution by Laser Scanning Confocal Microscopy

(LSCM)

To test the peroxisomal targeting ability of enhanced peroxisome targeting signal ePTS1, yeast cells expressing GFP-ePTS1 were cultured in 50 mL YPD medium for 24 h. For simultaneous visualization of GFP-ePTS1 and Nile red, precultures incubated in 50 mL YPD were stained by adding Nile red solution (1 mg/mL) in acetone to the cell suspension (0.1 v/v) and incubated for 60 min in the dark at room temperature. The stained cells were washed with normal saline and resuspended in potassium phosphate buffer (pH 7.4) before being transferred onto glass slides to visualize GFP at 488 nm and Nile red at 561 nm with an Olympus FV1000 confocal laser scanning microscope.

2.6. Esterification of the fermented supernatant

2 mL of the fermented supernatant was added to 1.5 mL of 10% HCl-CH_3OH solution, which was esterified at 62 ℃ for 3 h. Then, 2 mL of n-hexane was added and the resultant mixture was violently shaken for 1 min to dissolve the dimethyl itaconate. After centrifugation (6000 rpm, 5 min), the upper organic phase was transferred into another clean bottle for detection. Three 2 mL of 100 mg/L IA standard solutions were sampled for methyl esterification in accordance with this procedure, and these results analyzed by the GC-MS were compared with that of the 100 mg/L dimethyl itaconate standard substance.

2.7. GC-MS analysis

0.6 μL of the upper organic phase from section 2.6 was analyzed by GC–MS using an Agilent 7890A GC with a 5975C MSD equipped with an HP-5MS column (30 m ×0.25 mm ×0.25 μm, Agilent, Santa Clara, CA, USA). The GC oven temperature was initially held at 60 °C for 2 min, and then ramped up to 250 °C at a rate of 10 °C/min and held

for 9 min. The split ratio was 10:1. Helium was used as the carrier gas, with an inlet pressure of 13.8 psi. The injector was maintained at 250 °C and the ion source temperature was set to 220 °C. The final data analysis was performed using the Enhanced Data Analysis software (Agilent, Santa Clara, CA, USA) to obtain the standard curve of dimethyl itaconate, and the area obtained after the sample is analyzed and detected by the instrument is brought into the formula of the standard curve to obtain the output of dimethyl itaconate. The titer of IA is obtained by converting with the esterification rate obtained in 2.6.

2.8. Statistical analysis

Differences in titers between the control strain and other strains were evaluated using SPSS 22.0 software for Windows (SPSS, Chicago, IL, USA). One-way ANOVA analyses were carried out with a confidence interval of 95% and statistical significance between the groups and the relevant control was considered if P-value<0.05.

2.9. Bioreactor fermentations

Bioreactor fermentation was batch processed using an optimized medium formulation containing 59 g/L glucose, 16 g/L yeast extract and 8 g/L tryptone. The strain was first seeded in 50 mL YPD medium in 250 mL shake flasks, cultured at 30 °C and 220 rpm for 16 h. Following that, the bioreactor containing 3 L of YPO medium were inoculated with the seed cultures at an OD_{600} of 1.

Fermentation without any pH control was carried out in a 5 L stirred fermenter (Shanghai Baoxing Bioengineering Equipment Co., Ltd., Shanghai, China) at 30 °C and 1 vvm. The bioreactor pressure was maintained at 0.06 MPa. The impeller stirring speed was 400 rpm.

3. Results

3.1. Heterologous expression of A. terreus CAD in Y. lipolytica

In *A. terreus*, IA is generated from the decarboxylation of the TCA intermediate cis-aconitic acid by the CAD enzyme (Bonnarme et al., 1995). To test if *A. terrus's CAD* gene can be expressed successfully in *Y. lipolytica* without codon optimization, we first cloned the associated gene from *A. terreus* HAT418 strain into *Y. lipolytica* strain Po1g KU70Δ, with the gene's intron spliced out. In the gene sequencing analysis that followed, we discovered that the actual PCR-amplified gene sequence was different from the genome sequence shown in NCBI database. Our sequence data for *A. terreus* HAT418 *CAD* gene was submitted to GenBank under the accession number MT862134.1. Overexpression of the *CAD* gene in *Y. lipolytica* Po1g KU70Δ resulted in the creation of strain Po1g-CAD. We subjected both the engineered strain with cytosolic CAD and control strain without to shake flask fermentation and assayed for IA continuously over a period of 6 days. We confirmed that IA was produced only in the engineered *Y. lipolytica* but not in its wild type. IA levels were first detected in the supernatant on day 2 and they increased gradually with time, until a maximum yield of 33.12 mg/L was obtained on day 4 (Fig. 2). In all, our results implied that heterologous expression of the *A. terreus CAD* is required for stable IA production in *Y. lipolytica*.

3.2. Peroxisomal targeting of heterologous CAD gene improved IA production

β-oxidation of long chain fatty acids in eukaryotes are known to occur mainly in the peroxisomes (Wache et al., 2001; Hanko et al., 2018). In *Y. lipolytica,* this process produces acetyl-CoA which then enters the glyoxylate cycle for synthesis of the IA precursor, cis-aconitic acid (Dominguez et al., 2010; Koivistoinen et al., 2013; Xu et al., 2017). Several studies have shown that subcellular localization of specific enzymes

or metabolic pathways not only increase product conversion efficiency, but is also able to suppress the undesirable effects of competitive metabolic inhibition (Yang et al., 2019; Zhu et al., 2018; Zhu et al., 2021). As such, this approach of subcellular compartmentalization is adopted in our study and complemented with the use of WCO as the substrate to enable sustainable, efficient and low-cost production of IA. To this end, IA production from the glyoxylate cycle in *Y. lipolytica* was ensured by targeting the involved heterologous enzymes to the peroxisomal matrix through the addition of enhanced peroxisomal targeting signal (ePTS1) after its gene sequence. The ePTS1 applied in this instance has been shown to be localized in *S. cerevisiae* (DeLoache et al., 2016).

Two separate dyes, Nile red and green fluorescence, were employed for staining of the yeast cells to validate the peroxisomal targeting ability of ePTS1. In an earlier study, it was shown that hrGFPO, encoding the green fluorescence protein, was most strongly expressed in Po1g KU70Δ (Zhao et al., 2021a). The plasmid with sequence ePTS1 added after the hrGFPO protein sequence was retransformed into yeast, resulting in strain Po1g-hrGFPO-ePTS1 (Fig 3A). Nile red fluorescence, on the other hand, was used to stain the peroxisomes of the yeast cells. To determine if ePTS1 could be successfully localized to peroxisomes in *Y. lipolytica*, LSCM was performed to observe the location of the two different fluorescence in yeast cells. As shown in Fig 3B, a green fluorescent protein with localization signal ePTS1, which exhibits green light under microscope irradiation, was expressed in the engineered yeast. Yeast cells after Nile red staining also show localized red fluorescence under the microscope. Combining these two images, we observed that the green and red shades overlap almost completely and produce a bright yellow light. Therefore, it can be confirmed that ePTS1 plays a role in

261 determining the location of the peroxisome could be used as a peroxisomal targeting
262 sequence for *Y. lipolytica*.

263 Subsequently, the plasmid pYLEX1-CAD-ePTS1 constructed through the ligation of
264 ePTS1 downstream of the *CAD* gene was integrated into the *Y. lipolytica* Po1g KU70Δ
265 chromosomes of the strain. The resulting engineered strain was cultured in the YPO
266 medium and the 6-day time course of IA production titers and biomass were shown in
267 Fig. 4. The titers of IA increased continuously from the beginning of cultivation up to
268 day 4 with the highest titer having reached 1.58 g/L. Following this, the titers of IA
269 gradually stabilized, likely owing to WCO depletion. Notably, we also compared the
270 use of WCO and glucose in this subcellular compartmentalized approach to generate
271 IA under the same conditions. The use of WCO had resulted in almost 100-folds
272 increase in IA titer as compared to glucose (13.68 mg/L of IA) as the carbon source,
273 hence implying that WCO was superior to glucose for IA production in these
274 conditions. We also observed that the overproduction of IA has a positive effect on the
275 cell growth. Together, our results demonstrate that the the expression and localization
276 of *CAD* in the peroxisomes of *Y. lipolytica* can lead to substantial increase in IA
277 production.

278 ***3.3. Overexpression of endogenous genes involved in the acetyl-CoA production***
279 ***pathway of Y. lipolytica***

280 To further enhance IA production in *Y. lipolytica*, we attempted to study the pathway
281 genes involved in the conversion of oils to fatty acids and the utilization of fatty acids
282 to raise the flux of precursor acetyl-CoA. The β-oxidation of fatty acids is a four-
283 reaction cycle comprising of oxidation, hydration, dehydrogenation, and thiolysis,
284 which results in one molecule of acetyl-CoA released in the peroxisome (Braga et al.,

2016). In *Y. lipolytica*, the first step of fatty acid β-oxidation can be catalyzed by six different acyl-CoA oxidases (*POX1–6*) (Beopoulos et al., 2008). The second and third steps of β-oxidation were catalyzed by a multifunctional enzyme (*MFE1*) (Black et al., 2000; Dulermo et al., 2013), and the final step is catalyzed by peroxisomal thiolase (*POT1*) (Wang et al., 2020). As such, the genes involved in the β-oxidation pathway were overexpressed in an attempt to increase the flux towards IA. Ten genes, consisting of *LIP2* (encoding lipases, Zhang et al., 2021a), *POX1-6* (Ledesma-Amaro et al., 2016), *MEF1* (Haddouche et al., 2010), *POT1* (Smith et al., 2000), and *PEX10* (encoding a proteins required for peroxisome assembly, Zhang et al., 2021b), were overexpressed individually and investigated for their effects on IA overproduction to determine the genes critical for IA biosynthesis in the acetyl-CoA production pathway. To this end, ten strains were constructed on the basis of the strain expressing *CAD-ePTS1* gene, including the ten endogenous genes in the acetyl-CoA production pathway of *Y. lipolytica*; all genes were integrated into the chromosome of *Y. lipolytica* Po1g KU70Δ. These ten engineered strains were then cultured in YPO medium for 6 days in shake flasks. The IA titers of the strains showed that the overexpression of the individual corresponding genes could improve IA production compared to the control strains expressing only the respective *CAD-ePTS1* gene. Among them, the POT1-overexpressed strains (hereafter named Po1g-2G), achieved the highest titers of 2.42 g/L for IA after 4 days of cultivation (Fig. 5). The results indicated that overexpression of these key enzymes can effectively promote the fatty acid degradation process and release the most acetyl-CoA molecules for IA biosynthesis. This observation is consistent with several other studies in which *POT1* has already been demonstrated to be the key rate-limiting enzyme in the β-oxidation pathway (Ma et al., 2020; Zhang et al., 2021b). Therefore, the engineered strain Po1g-2G was used for subsequent

engineering efforts to boost IA production.

3.4. Effects of deletion of the CAT and ICL genes on IA production in Y. lipolytica.

The yield of IA can be further improved by reducing the loss of the precursor acetyl-CoA and preventing the synthesis of cis-aconitic acid from the glyoxylate cycle into downstream products such as succinic acid. The carnitine acetyltransferases (*CAT*) gene is responsible for transporting acetyl-CoA between different organelles, which can reversibly link the acetyl units to the carrier molecule carnitine (Strijbis et al., 2010; Strijbis et al., 2008). Meanwhile, the isocitrate lyase (*ICL*) gene manages the conversion of isocitrate into succinic acid and glyoxylic acid (Koivistoinen et al., 2013). To verify if either of these genes assume a major role in IA production, both genes singly were deleted from Po1g KU70Δ, resulting in the creation of strains Po1g-2G-CATΔ and Po1g-2G-ICLΔ. After cultivating the resulting strains in shake flasks in YPO medium, we found that higher IA production up to 3.33 g/L was observed in ICL knockout strain as compared to CAT knockout strain with 2.8 g/L titers. This suggests that blocking the downstream pathway improves IA production while blocking the efflux effect of the acetyl coenzyme in the peroxisome is not as advantageous. Thus, the Po1g-2G-ICLΔ strain was selected as the final optimized strain.

3.5. IA production by the engineered Y. lipolytica in bioreactor

One of the most crucial issues in platform chemicals production is in achieving high product titers consistently (Gao et al., 2016). To investigate the performance of IA-producing *Y. lipolytica* at conditions that are more relevant for large-scale application, a 5L bioreactor was employed. Unlike the procedure conducted in the shaking flask fermentation method, here, the composition of the growth medium was altered and the approach of adding sufficient WCO substrate at the onset was adopted to avoid the

problems caused by fed batch fermentation. In the phase of active cell growth between 24 to 96 hours, the Po1g-2G-ICLΔ strain intensively produced IA. During this period, the average specific rate of citric acid synthesis was 0.8 g/L/h, and the maximum specific rate of 2.3 g/L/h was observed between the 76 to 96-hour intervals (Fig. 6). Hence, the maximum yield of IA was 54.55 g/L after the 96-hour reaction in the fermenter. At the time of writing, this is the highest IA production achieved by a yeast host reported worldwide. As such, *Y. lipolytica* would be a promising industrial host for IA production from renewable feedstock. Our study also demonstrated that the circular bioeconomy concept can be an effective model for scale-up production of valuable biochemical, in particular with the valorization of WCO as raw material.

4. Discussion

With increasing global interest in environmental protection and sustainable development, the use of low-cost waste to produce valuable platform chemicals in the industrial scale is gaining attention. In the few studies conducted to date, IA production in engineered strains of *Y. lipolytica* were predominantly using glucose as the primary carbon source (Blazeck et al., 2015; Zhao et al., 2019).. Even so, production titers had remained suboptimal (Table 1). This had limited the feasibility of large-scale industrial adoption. Here, we employed the cheap raw material WCO to increase acetyl-CoA availability for conversion into IA in the peroxisomes of *Y. lipolytica*. By applying both systems metabolic engineering and bioprocessing optimization strategies in unison, we achieved IA titers of 3.33 g/L in shake flasks and up to 54.55 g/L in stirred-tank bioreactor on WCO as the carbon source without the need for pH control. This amounted to more than 34-folds as compared to the initial titers of 1.58 g/L IA before the optimization of strain and fermentation conditions. In this study, as the supernatant

may contain WCO that was not consumed completely, IA cannot be detected directly by HPLC. We used esterification of the supernatant to detect the yield of dimethyl itaconate. While this method, in principle, can be used to determine the theoretical final yield of IA from the esterification rate, it is not the best approach to quantify the exact yield of IA. The development of a more robust and higher throughput method of analysis should be considered in future studies. Furthermore, the yield of organic acids produced by *Y. lipolytica* is primarily affected by the genetic mechanism and various environmental factors, such as the carbon source, nitrogen source, temperature, pH, iron concentration, and dissolved oxygen levels. As such, since bioreactor fermentation with WCO as the sole carbon source is still relatively understudied, further optimization of the fermentation conditions could improve IA yields. Nonetheless, the present work on the production of IA by WCO still provides valuable insights that will facilitate further efforts in the biosynthesis of this compound. The results obtained suggest that the oleaginous yeast *Y. lipolytica* is an attractive platform as it provides a viable and scalable pathway to the overproduction of IA and most notably, one that is sustained by waste conversion. However, given the extensive knowledge on IA gene regulation and fermentation conditions, it is believed that higher productivities of IA can be achieved through further engineering of the yeast strain and the optimization of fermentation conditions in subsequent studies.

Ethics approval and consent to participate

This manuscript does not contain any studies with human participants or animals performed by any of the authors.

Consent for publication

All authors give consent to publish the research in *Frontiers in Bioengineering and Biotechnology*.

Availability of data and material

All relevant data generated and analyzed during this study are included in this manuscript. Correspondence to authors is welcomed.

Conflict of interests

The authors declare that the research was conducted in the absence of any commercial or financial relationships that could be construed as a potential conflict of interest.

Authors' contributions

DGX, CYZ, AW and AQY conceived and designed the study. LXR, LM, SHW, YPW, SQL, ZHL and BXZ performed the experiments. LXR and KP analyzed data and wrote the manuscript. DGX, CYZ, AW and AQY critically revised the manuscript. All authors have read and approved the final manuscript.

Acknowledgments

This work was supported by the Natural Science Foundation of Tianjin, China (17JCYBJC40800), the Research Foundation of Tianjin Municipal Education Commission, China (2017ZD03), the Innovative Research Team of Tianjin Municipal

Education Commission, China (TD13-5013), Tianjin Municipal Science and Technology Project (18PTSYJC00140, 19PTSYJC00060), Startup Fund for 'Haihe Young Scholars' of Tianjin University of Science and Technology, the Thousand Young Talents Program of Tianjin, China. AW was supported by the Ministry of Education, Singapore (R-MOE-A401-F028) and Lee Foundation (T-LEE-T201-A001).

Authors' information

[1]State Key Laboratory of Food Nutrition and Safety, Key Laboratory of Industrial Fermentation Microbiology of the Ministry of Education, Tianjin Key Laboratory of Industrial Microbiology, College of Biotechnology, Tianjin University of Science and Technology, No.29 the 13th Street TEDA, Tianjin 300457, PR China

[2]Food, Chemical and Biotechnology Cluster, Singapore Institute of Technology, Singapore 138683, Singapore

References

Beopoulos, A., Mrozova, Z., Thevenieau, F., Le-Dall, M. T., Hapala, I., Papanikolaou, S., et al. (2008). Control of lipid accumulation in the yeast *Yarrowia lipolytica*. *Appl. Environ. Microbiol*. 74(24), 7779-7789. doi: 10.1128/AEM.01412-08

Black, P. N., Faergeman, N. J, and DiRusso, C. C. (2000). Long-chain acyl-CoA-dependent regulation of gene expression in bacteria, yeast and mammals. *J. Nutr*. 130(2S Suppl), 305S-309S. doi: 10.1093/jn/130.2.305S

Blazeck, J., Miller, J., Pan, A., Gengler, J., Holden, C., Jamoussi, M., et al. (2014). Metabolic engineering of *Saccharomyces cerevisiae* for itaconic acid production. *Appl. Microbiol. Biotechnol.* 98, 8155-8164. doi: 10.1007/s00253-014-5895-0

Blazeck, J., Hill, A., Jamoussi, M., Pan, A., Miller, J., Alper, H. S. (2015). Metabolic engineering of *Yarrowia lipolytica* for itaconic acid production. *Metab. Eng*. 32, 66-73. doi: 10.1016/j.ymben.2015.09.005

Bonnarme, P., Gillet, B., Sepulchre, A. M., Role, C., Beloeil, J. C., and Ducrocq, C. (1995). Itaconate biosynthesis in *Aspergillus terreus*. *J. Bacteriol*. 177(12), 3573-3578. doi: 10.1128/jb.177.12.3573-3578

Braga, A., and Belo, I. (2016). Biotechnological production of γ-decalactone, a peach like aroma, by *Yarrowia lipolytica*. *World. J. Microbiol. Biotechnol*. 32(10), 169. doi: 10.1007/s11274-016-2116-2

Cui, Z. Y., Gao, C. J., Li, J. J., Hou, J., Lin, C. S. K., and Qi, Q. S. (2017). Engineering of unconventional yeast *Yarrowia lipolytica* for efficient succinic acid production from glycerol at low pH. *Metab. Eng*. 42, 126-133. doi: 10.1016/j.ymben.2017.06.007

De-Hoog, G. S.(1996). Risk assessment of fungi reported from humans and animals. *Mycoses*. 39(11-12), 407-417. doi: 10.1111/j.1439-0507.1996.tb00089.x

DeLoache, W. C., Russ, Z. N., and Dueber, J. E. (2016). Towards repurposing the yeast peroxisome for compartmentalizing heterologous metabolic pathways. *Nat. Commun*. 7, 11152. doi: 10.1038/ncomms11152

Dominguez, A., Deive, F. J., Sanroma´n, M. A., and Longo, M. A. (2010). Biodegradation and utilization of waste cooking oil by *Yarrowia lipolytica* CECT 1240. *Eur. J. Lipid. Sci. Technol*. 112, 1200-1208. doi: 10.1002/ejlt.201000049

Dulermo, T., Tréton, B., Beopoulos, A., Gnankon, A. P. K., Haddouche, R., and Nicaud, J. M. (2013). Characterization of the two intracellular lipases of *Y. lipolytica* encoded by TGL3 and TGL4 genes: new insights into the role of intracellular lipases and lipid body organisation. *Biochim. Biophys. Acta*. 1831(9), 1486-1495. doi: 10.1016/j.bbalip.2013.07.001

Gao, C. J., Yang, X. F., Wang, H., Rivero, C. P., Li, C., Cui, Z. Y., et al. (2016). Robust succinic acid production from crude glycerol using engineered *Yarrowia lipolytica. Biotechnol. Biofuels*. 9(1), xz2179. doi: 10.1186/s13068-016-0597-8

Geiser, E., Przybilla, S. K., Friedrich, A., Buckel, W., Wierckx, N., Blank, L. M., et al. (2016). *Ustilago maydis* produces itaconic acid via the unusual intermediate trans-aconitate. *Microb. Biotechnol*. 9(1), 116-126. doi: 10.1111/1751-7915.12329

Gonçalves, F. A., Colen, G., and Takahashi, J. A. (2014). *Yarrowia lipolytica* and its multiple applications in the biotechnological industry. *Scientific. World. Journal*. 2014, 476207. doi: 10.1155/2014/476207

Haddouche, R., Delessert, S., Sabirova, J., Neuvéglise, C., Poirier, Y., and Nicaud, J. M. (2010). Roles of multiple acyl-CoA oxidases in the routing of carbon flow towards β-oxidation and polyhydroxyalkanoate biosynthesis in *Yarrowia lipolytica*. *FEMS. Yeast. Res*. 10(7), 917-927. doi: 10.1111/j.1567-1364.2010.00670.x

Hanko, E. K. R., Denby, C. M., Nogué, V. S. I. , Lin, W. Y., Ramirez, K. J., Singer, C. A., et al. (2018). Engineering β-oxidation in *Yarrowia lipolytica* for methyl ketone production. *Metab. Eng*. 48, 52-62. doi: 10.1016/j.ymben.2018.05.018

Harder, B. J., Bettenbrock, K., and Klamt, S. (2016). Model-based metabolic engineering enables high yield itaconic acid production by *Escherichia coli. Metab. Eng*. 38, 29-37. doi: 10.1016/j.ymben.2016.05.008

Koivistoinen, O. M., Kuivanen, J., Barth, D., Turkia, H., Pitkänen, J. P., Penttilä, M., et al. (2013). Glycolic acid production in the engineered yeasts *Saccharomyces cerevisiae* and *Kluyveromyces lactis. Microb. Cell. Fact*. 12, 82. doi: 10.1186/1475-2859-12-82

Krull, S., Hevekerl, A., Kuenz, A., and Prüße, U. (2017). Process development of itaconic acid production by a natural wild type strain of *Aspergillus terreus* to reach industrially relevant final titers. *Appl. Microbiol. Biotechnol*. 101(10), 4063-4072. doi: 10.1007/s00253-017-8192-x

Kubicek, C. P., Punt, P., and Visser, J. (2011). Production of organic acids by filamentous fungi. *Springer*.10, 215-234. doi: 10.1007/978-3-642-11458-8_10

Kuenz, A., Gallenmüller, Y., Willke, T., and Vorlop, K. D. (2012). Microbial production of itaconic acid: developing a stable platform for high product concentrations. *Appl. Microbiol. Biotechnol*. 96(5), 1209-1216. doi: 10.1007/s00253-012-4221-y

Ledesma-Amaro, R., and Nicaud, J. M. (2016). *Yarrowia lipolytica* as a biotechnological chassis to produce usual and unusual fatty acids. *Prog. Lipid. Res*. 61, 40-50. doi: 10.1016/j.plipres.2015.12.001

Li, J., Rong, L. X., Zhao, Y., Li, S. L., Zhang, C. Y., Xiao, D. G., et al. (2020). Next-generation metabolic engineering of non-conventional microbial cell factories for carboxylic acid platform chemicals. *Biotechnol. Adv*. 43, 107605. doi: 10.1016/j.biotechadv.2020.107605

Li, J., Zhu, K., Miao, L., Rong, L. X., Zhao, Y., Li, S. L., et al. (2021). Simultaneous improvement of limonene production and tolerance in *Yarrowia lipolytica* through tolerance engineering and evolutionary engineering. *ACS. Synth. Biol*. 10, 884-896. doi: 10.1021/acssynbio.1c00052

Li, S. L., Rong, L. X., Wang, S. H., Liu, S. Q., Lu, Z. H., Miao, L., et al. (2022). Enhanced limonene production by metabolically engineered *Yarrowia lipolytica* from cheap carbon sources. *Chem. Eng. Sci*. 249, 117342. doi: 10.1016/j.ces.2021.117342

Liu, H. H., Ji, X. J., and Huang, H. (2015). Biotechnological applications of *Yarrowia lipolytica*: past, present and future. *Biotechnol. Adv*. 33(8), 1522-1546. doi: 10.1016/j.biotechadv.2015.07.010

Ma, Y. R., Li, W. J., Mai, J., Wang, J. P., Wei, Y. J., Ledesma-Amaro, R., et al. (2020). Engineering *Yarrowia lipolytica* for sustainable production of the chamomile sesquiterpene (−)-α-bisabolol. *Green. Chem.* 23, 780-787. doi: 10.1039/d0gc03180a

Ng, T. K., Yu, A. Q., Ling, H., Juwono, N. K. P., Choi, W. J., Leong, S. S. J., et al. (2020). Engineering *Yarrowia lipolytica* towards food waste bioremediation: production of fatty acid ethyl esters from vegetable cooking oil. *J. Biosci. Bioeng*. 129(1), 31-40. doi: 10.1016/j.jbiosc.2019.06.009

Nuss, P., and Gardner, K. H. (2013). Attributional life cycle assessment (ALCA) of polyitaconic acid production from northeast US softwood biomass. *Int. J. Life. Cycle. Assess*. 18, 603–612. doi: 10.1007/s11367-012-0511-y

Okamoto, S., Chin, T., Hiratsuka, K., Aso, Y., Tanaka, Y., Takahashi, T., et al. (2014). Production of itaconic acid using metabolically engineered *Escherichia coli*. *J. Gen. Appl. Microbiol.* 60(5), 191-7. doi: 10.2323/jgam.60.191

Otten, A., Brocker, M., and Bott, M. (2015). Metabolic engineering of *Corynebacterium glutamicum* for the production of itaconate. *Metab. Eng*. 30, 156-165. doi: 10.1016/j.ymben.2015.06.003

Pang, Y. R., Zhao, Y. K., Li, S. L., Zhao, Y., Li, J., Hu, Z. H., et al. (2019). Engineering the oleaginous yeast *Yarrowia lipolytica* to produce limonene from waste cooking oil. *Biotechnol. Biofuels*. 12, 241. doi: 10.1186/s13068-019-1580-y

Porro, D., and Branduardi, P. (2017). Production of organic acids by yeasts and filamentous fungi. *Biotechnol Yeasts Filamentous Fungi*. 14, 205-223. doi: 10.1007/978-3-319-58829-2_7

Smith, J. J., Brown, T. W., Eitzen, G. A., and Rachubinski, R. A. (2000). Regulation of peroxisome size and number by fatty acid beta-oxidation in the yeast *Yarrowia lipolytica*. *J. Biol. Chem.* 275(26), 20168-20178. doi: 10.1074/jbc.M909285199

Sriariyanun, M., Heitz, J. H., Yasurin, P., Asavasanti, S., and Tantayotai, P. (2019). Itaconic acid: a promising and sustainable platform chemical? *Appl. Science. Eng. Prog.* 12(1), 14410-14416. doi: 10.14416/j.asep.2019.05.002

Strijbis, K., van-Roermund, C. W., van-den Burg, J., van-den Berg, M., Hardy, G. P., Wanders, R. J., et al. (2010). Contributions of carnitine acetyltransferases to intracellular acetyl unit transport in *Candida albicans. J. Biol. Chem*. 285(32), 24335-24346. doi: 10.1074/jbc.M109.094250

Strijbis, K., van-Roermund, C. W., Visser, W. F., Mol, E. C., van-den Burg, J.,

MacCallum, D. M. (2008). Carnitine-dependent transport of acetyl coenzyme A in *Candida albicans* is essential for growth on nonfermentable carbon sources and contributes to biofilm formation. *Eukaryot. Cell*. 7(4), 610-618. doi: 10.1128/EC.00017-08

Sun, W., Vila-Santa, A., Liu, N., Prozorov, T., Xie, D. M., Faria, N. T., et al. (2020). Metabolic engineering of an acid-tolerant yeast strain *Pichia kudriavzevii* for itaconic acid production. *Metab. Eng. Commun.* 10, e00124. doi: 10.1016/j.mec.2020.e00124

Tehrani, H. H., Becker, J., Bator, I., Saur, K., Meyer, S., Rodrigues Lóia, A. C., et al. (2019a). Integrated strain and process design enable production of 220 g/L itaconic acid with *Ustilago maydis. Biotechnol. Biofuels*. 12, 263. doi: 10.1186/s13068-019-1605-6

Tehrani, H. H., Tharmasothirajan, A., Track, E., Blank, L. M., and Wierckx, N. (2019b). Engineering the morphology and metabolism of pH tolerant *Ustilago cynodontis* for efficient itaconic acid production. *Metab. Eng*. 54, 293-300. doi: 10.1016/j.ymben.2019.05.004

Tevz, G., Bencina, M., and Legisa, M. (2010). Enhancing itaconic acid production by *Aspergillus terreus*. *Appl. Microbiol. Biotechnol*. 87(5), 1657-1664. doi: 10.1007/s00253-010-2642-z

Vuoristo, K. S., Mars, A. E., Sangra, J. V., Springer, J., Eggink, G., Sanders, J. P., et al. (2015). Metabolic engineering of itaconate production in *Escherichia coli*. *Appl. Microbiol. Biotechnol*. 99(1), 221-8. doi: 10.1007/s00253-014-6092-x

Wache, Y., Aguedo, M., Choquet, A., Gatfield, I. L., Nicaud, J. M., and Belin, J. M. (2001). Role of beta-oxidation enzymes in gamma-decalactone production by the yeast *Yarrowia lipolytica. Appl. Environ. Microbiol*. 67(12), 5700-5704. doi: 10.1128/AEM.67.12.5700-5704.2001

Wang, J.P., Ledesma-Amaro, R., Wei, Y. J., Ji, B. Y., and Ji, X. J. (2020). Metabolic engineering for increased lipid accumulation in *Yarrowia lipolytica* - A Review. *Bioresour. Technol*. 313, 123707. doi: 10.1016/j.biortech.2020.123707

Werpy, T., and Petersen, G. (2004). Top Value Added Chemicals from Biomass: Volume IResults of Screening for Potential Candidates from Sugars and Synthesis Gas. National Renewable Energy Lab., Golden, CO (US).

Willke, T. and Vorlop, K. D. (2001). Biotechnological production of itaconic acid. *Appl*. *Microbiol*. *Biotechnol*., **56**, 289– 295. doi: 10.1007/s002530100685

Xu, P., Qiao, K. J., and Stephanopoulos, G. (2017). Engineering oxidative stress defense pathways to build a robust lipid production platform in *Yarrowia lipolytica. Biotechnol. Bioeng*. 114(7), 1521-1530. doi: 10.1002/bit.26285

Yang, K. X., Qiao, Y. G., Li, F., Xu, Y., Yan, Y. J., Madzak, C., et al. (2019). Subcellular engineering of lipase dependent pathways directed towards lipid related organelles for highly effectively compartmentalized biosynthesis of triacylglycerol derived products in *Yarrowia lipolytica. Metab. Eng*. 55, 231-238. doi: 10.1016/j.ymben.2019.08.001

Yu, A. Q., Pratomo, N., Ng, T. K., Ling, H., Cho, H. S., Leong, S. S., et al. (2016). Genetic engineering of an unconventional yeast for renewable biofuel and biochemical production. *J. Vis. Exp.* 115, 54371. doi: 10.3791/54371

Zhao, C., Cui, Z. Y., Zhao, X. Y., Zhang, J. X., Zhang, L. H., Tian, Y. J., et al. (2019). Enhanced itaconic acid production in *Yarrowia lipolytica* via heterologous expression of a mitochondrial transporter MTT. *Appl. Microbiol. Biotechnol*. 103(5), 2181-2192. doi: 10.1007/s00253-019-09627-z

Zhao, M., Lu, X. Y., Zong, H., Li, J. Y., and Zhuge, B. (2018). Itaconic acid production in microorganisms. *Biotechnol. Lett*. 40(3), 455-464. doi: 10.1007/s10529-017-2500-5

Zhao, Y., Liu, S. Q., Lu, Z. H., Zhao, B. X., Wang, S. H., and Zhang, C. Y. (2021a). Hybrid promoter engineering strategies in *Yarrowia lipolytica*: isoamyl alcohol production as a test study. *Biotechnol. Biofuels*. 14(1), 149. doi: 10.1186/s13068-021-02002-z

Zhao, Y. K., Zhu, K., Li, J., Zhao, Y., Li, S. L., Zhang, C. Y., et al. (2021b). High-efficiency production of bisabolene from waste cooking oil by metabolically engineered *Yarrowia lipolytica. Microb. Biotechnol*. 14(6), 2497-2513. doi: 10.1111/1751-7915.13768

Zhang, J., Jin, B., Hong, K. Q., Lv, Y., Wang, Z. W., and Chen, T. (2021a). Cell catalysis of citrate to itaconate by engineered *Halomonas bluephagenesis. ACS. Synth. Biol*. 13, 33-39. doi: 10.1021/acssynbio.1c00320

Zhang, Q., Yu, S.Q., Lyu, Y. B., Zeng, W. Z., and Zhou, J. W. (2021b). Systematically engineered fatty acid catabolite pathway for the production of (2S)-Naringenin in *Saccharomyces cerevisiae. ACS. Synthetic. Biology*. 10(5), 1166–1175. doi: 10.1021/acssynbio.1c00002

Zhou, J. W., Yin, X. X., Madzak, C., Du, G. C., and Chen, J. (2012). Enhanced α-ketoglutarate production in *Yarrowia lipolytica* WSH-Z06 by alteration of the acetyl-CoA metabolism. *J. Biotechnol*. 161(3), 257-264. doi: 10.1016/j.jbiotec.2012.05.025

Zhu, J., Schwartz, C., and Wheeldon, L. (2018). Controlled intracellular trafficking alleviates an expression bottleneck in *S. cerevisiae* ester biosynthesis. *Metab. Eng. Commun*. 8, e00085. doi: 10.1016/j.mec.2018.e00085

Zhu, K., Kong, J., Zhao, B. X., Rong, L. X., Liu, S. Q., Lu, Z. H., et al. (2021). Metabolic engineering of microbes for monoterpenoid production. *Biotechnol. Adv*. 53, 107837. doi: 10.1016/j.biotechadv.2021.107837

Zinjarde, S. S. (2014). Food-related applications of *Yarrowia lipolytica. Food. Chem*. 152, 1-10. doi: 10.1016/j.foodchem.2013.11.117

601 **Table 1 Representative examples of IA production in engineered microbial hosts**

Parental strain	Engineering strategy	Fermentation condition	Carbon Source	Titer	Reference
E. coli	*CAD*↑, *CS*↑, *ICD*↓, *ICL*Δ, *PTA*Δ, *PYK*Δ, *SUCS*Δ	Fed-batch bioreactor	Glucose and glutamic acid	32.00 g/L	Harder et al., 2016
	CAD↑, *ACO*↑, *ICD*Δ	Fed-batch bioreactor	LB+Glucose	4.34 g/L	Okamoto et al., 2014
	CAD↑, *CS*↑, *ACO*↑, *PTA*Δ, *LDH*Δ	Bioreactor	LB+Glucose	0.69 g/L	Vuoristo et al., 2015
S. cerevisiae	*CAD*↑, *ADE3*Δ, *BNA2*Δ, *TES1*Δ	Large-scale bioreactor	Glucose	0.17 g/L	Blazeck et al., 2014
Halomonas bluephagenesis	*CAD*↑, *ACO*↑, *ICD*↓	Batch shake flask	Citrate	63.60 g/L	Zhang et al., 2021
Corynebacterium glutamicum	*CAD*↑, *MALE*↑, *ICD*↓	Shake flask	Glucose	7.80 g/L	Otten et al., 2015
Pichia kudriavzevii	*CAD*↑, MTT↑, *ICD*Δ	Fed-batch bioreactor	Glucose	1.23 g/L	Sun et al., 2020
Y. lipolytica	*CAD*↑, *ACO*↑, *AMPD*↓	Bioreactor	Glucose	4.60 g/L	Blazeck et al., 2015
	CAD↑, MTT↑	Fed-batch bioreactor	Glucose	22.02 g/L	Zhao et al., 2019
	CAD-ePTS1↑, *POT1*↑, *ICL*Δ	Bioreactor	Waste cooking oil	54.55 g/L	This study

602 ↑ Gene overexpression; ↓ Gene knockdown; Δ Gene knockout; ***CAD*** cis-aconitic acid

603 decarboxylase; ***CS*** citrate synthase; ***ICD*** isocitrate dehydrogenase; ***ICL*** isocitrate lyase;

PTA phosphate acetyltransferase; ***PYK*** pyruvate kinase; ***SUCS*** succinyl-CoA synthetase; ***ACO*** aconitase; ***LDH*** lactate dehydrogenase; ***ADE3*** cytoplasmic trifunctional C1-tetrahydrofolate (THF) synthase; ***BNA2*** a putative tryptophan 2,3-dioxygenase or indoleamine 2,3-dioxygenase; ***TES1*** peroxisomal acyl-CoA thioesterase; **MALE** maltose-binding protein; **MTT** mitochondrial tricarboxylate transporter; ***AMPD*** adenosine monophosphate deaminase; *POT1* peroxisomal thiolase.

Figure legends

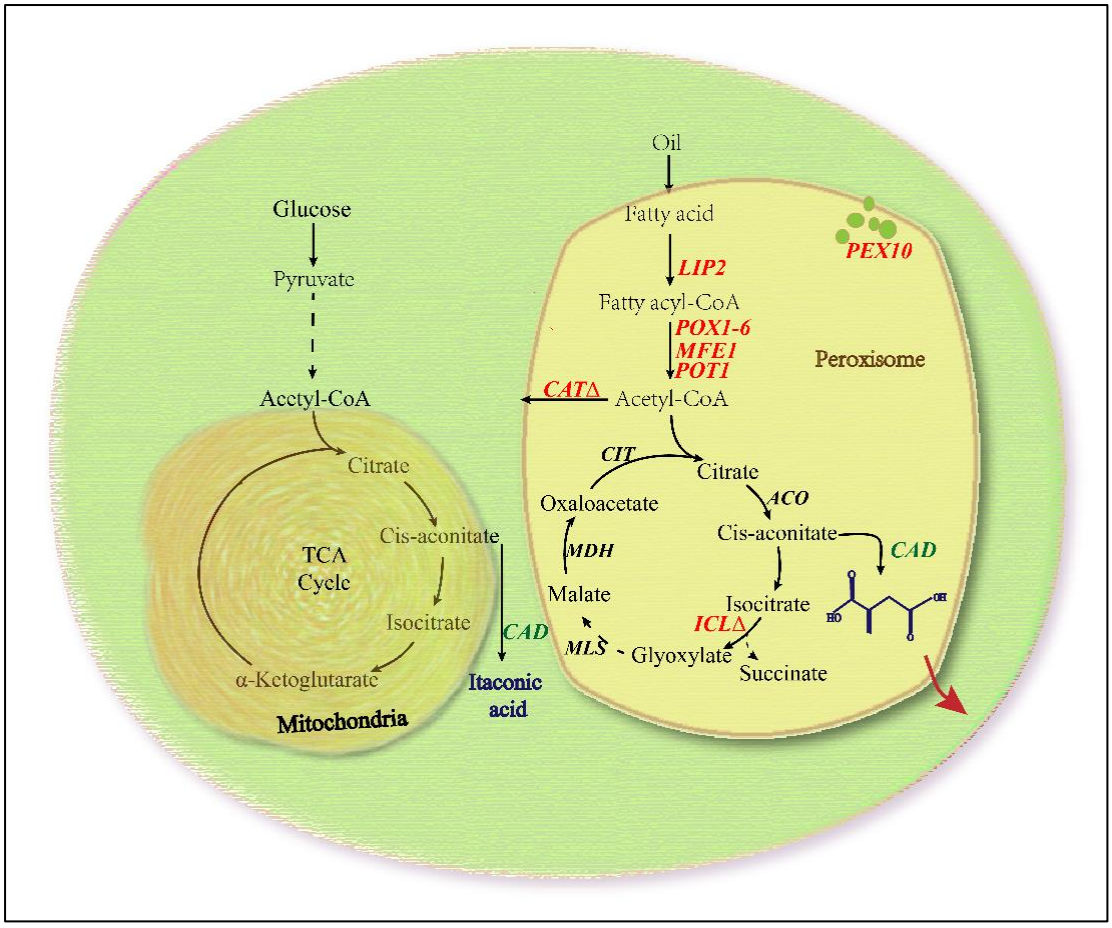

Figure 1. Simplified schematic of IA biosynthetic pathway in *Y. lipolytica*. Engineered *Y. lipolytica* uptakes and converts extracellular carbon sources such as glucose and waste cooking oil into IA products. Genes and metabolites of the native TCA and glyoxylate cycle pathway are identified in black, while heterologously introduced genes are shown in green and the endogenous genes used in this paper are shown in red. LIP2: lipases, POX1-6: six diffffferent acyl-CoA oxidases, MFE1: multifunctional enzyme, POT1: peroxisomal thiolase, PEX10: a proteins required for peroxisome assembly, CAT: carnitine acetyltransferases, ICL: isocitrate lyase, CAD: iso-aconitic acid decarboxylase, ACO: aconitase, MLS: malate synthase, MDH: malate dehydrogenase, CIT: citrate synthase.

623

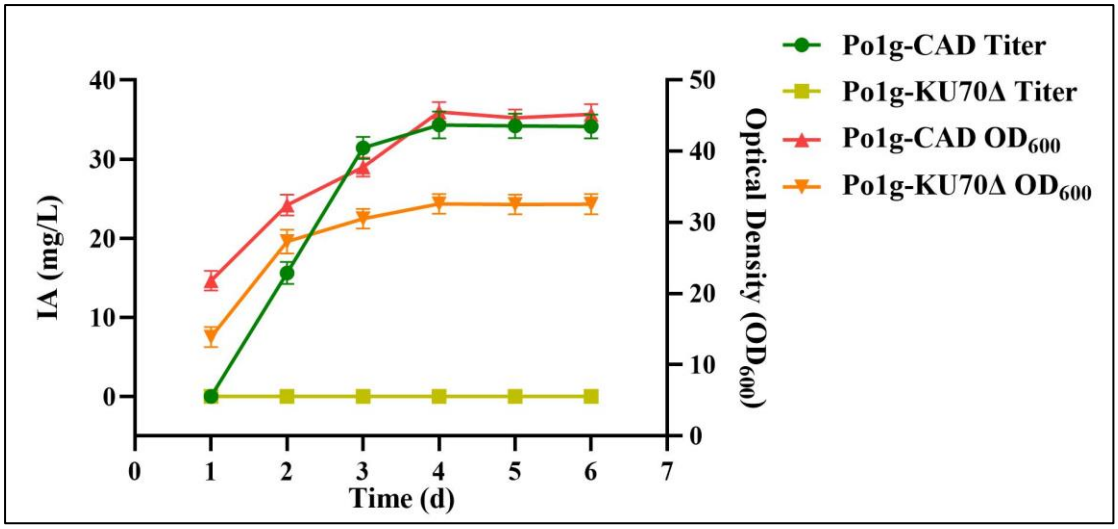

624 **Figure 2. IA production in *Y. lipolytica* strains expressing the *CAD* gene.** The titer
625 of IA and biomass were determined by shaking flask fermentation of Po1g-CAD strain
626 and control strain Po1g in YPO culture. All values presented are the mean of three
627 biological replicates ± standard deviation.

628

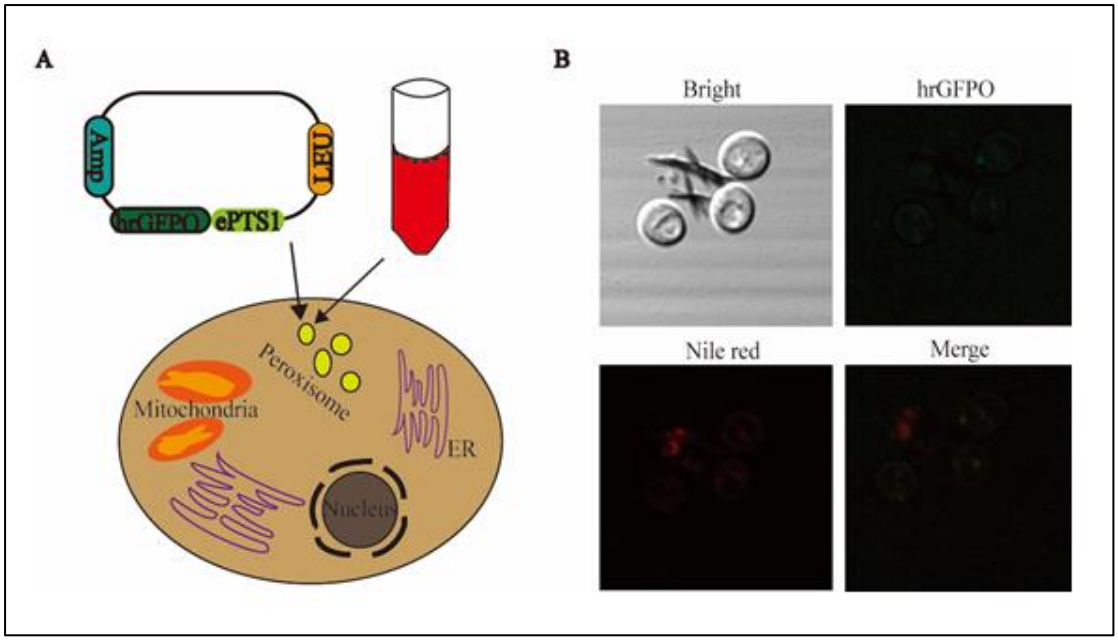

629

630 **Figure 3. Investigation of the localization of peroxisomes.** (A) Schematic diagram of
631 experimental design. GFP-ePTS1 is used to specifically mark peroxisomes in *Y.*
632 *lipolytica*. Nile red is used to show intracellular peroxisomes regions. (B) Localization
633 observation of peroxisomes use the Nile red and strain Po1g-hrGFPO-ePTS1 through
634 LSCM.

635

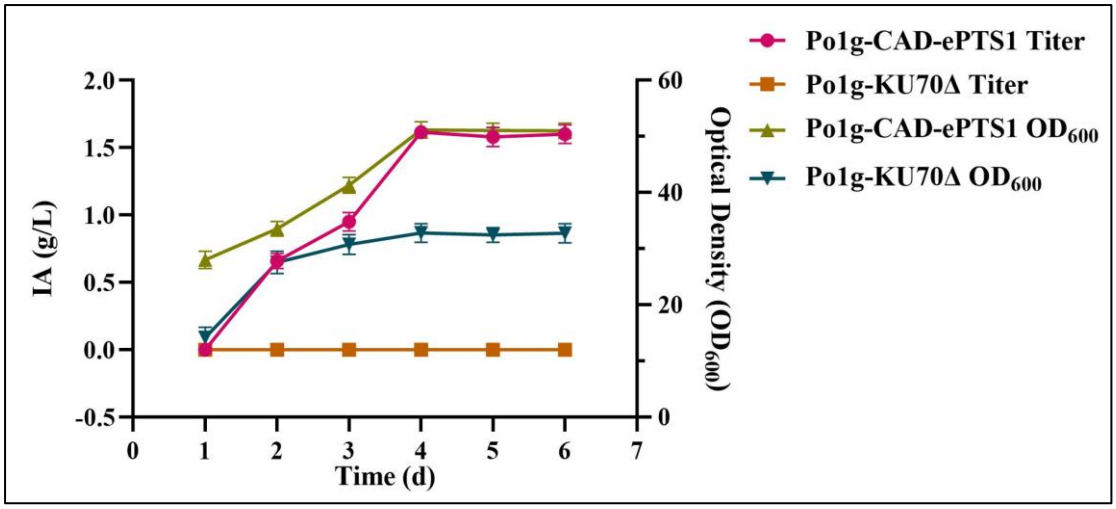

636

637 **Figure 4. IA production in *Y. lipolytica* strains expressing the CAD-ePTS1 gene.**

638 The titer of IA and biomass were determined by shaking flask fermentation of Po1g-

639 CAD-ePTS1 strain and control strain Po1g in YPO culture. All values presented are the

640 mean of three biological replicates ± standard deviation.

641

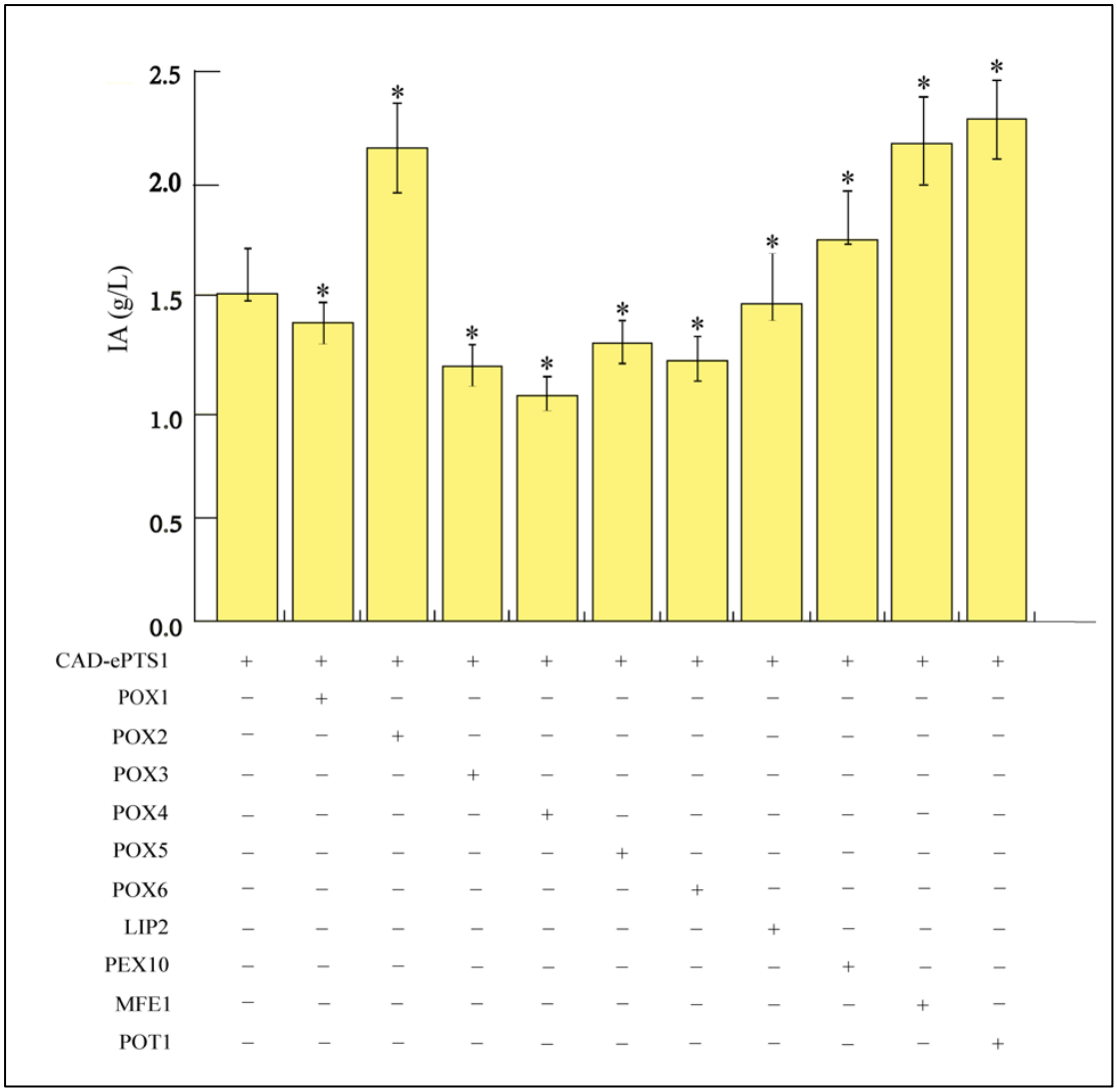

642

643 **Figure 5. Effects of overexpressing genes involved in the acetyl-CoA production**
644 **pathway on IA production.** The genes involved in the acetyl-CoA production pathway,
645 consisting of *LIP2, POX1-6, MFE1, POT1* and *PEX10,* were overexpressed
646 individually. Titers of IA produced by the strains were quantified after 6 days of
647 cultivation in shake flasks with YPO medium. All values presented are the mean of
648 three biological replicates ± standard deviation. *P<0.05, significantly different from
649 control by ANOVA.

650

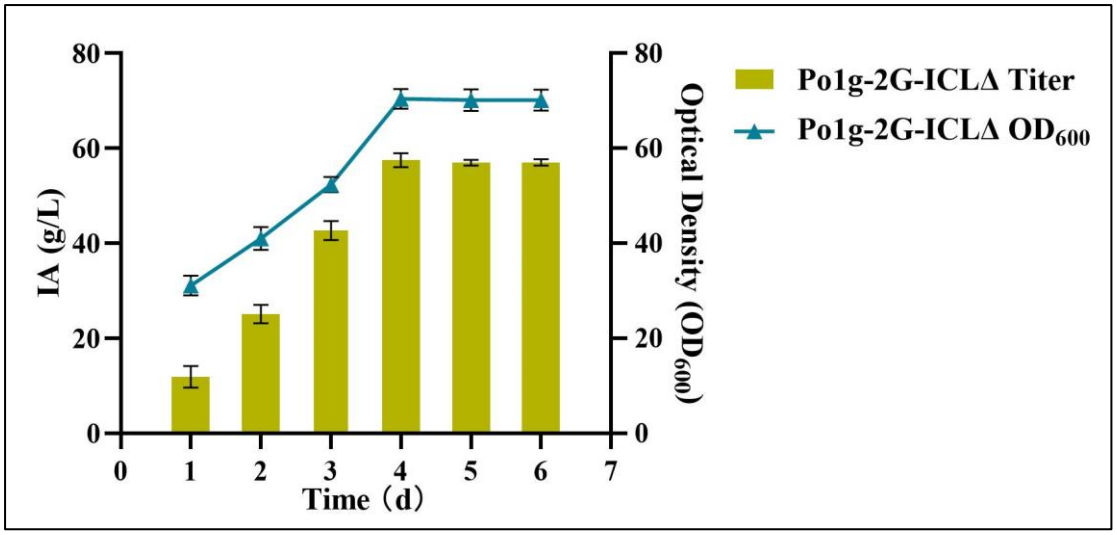

Figure 6. IA production in bioreactor of *Y. lipolytica* strain expressing the 2G-ICLΔ gene. The titer of IA and biomass were determined by bioreactor fermentation of Po1g-2G-ICLΔ strain in YPO culture. All values presented are the mean of three biological replicates ± standard deviation.

SUPPLEMENTARY INFORMATION

Engineering *Yarrowia lipolytica* to produce itaconic acid from waste cooking oil

Lanxin Rong[1], Lin Miao[1], Shuhui Wang[1], Yaping Wang[1], Shiqi Liu[1], Zhihui Lu[1], Baixiang Zhao[1], Cuiying Zhang[1], Dongguang Xiao[1], Krithi Pushpanathan[2], Adison Wong[2*], Aiqun Yu[1*]

SUPPLEMENTARY TABLES

Table S1. Plasmids and strains of used in this study

Plasmids	Features	Reference
pYLEX1	*Y. lipolytica*-integrative plasmid, Php4d-TXPR2, LEU2	Li jian
pYLEX1-CAD	P_{hp4d}-CAD-T_{XPR2}, LEU2	This study
pYLEX1-hrGFPO-ePTS1	P_{hp4d}-hrGFPO-ePTS1-T_{XPR2}, LEU2	This study
pYLEX1-CAD-ePTS1	P_{hp4d}-CAD-ePTS1-T_{XPR2}, LEU2	This study
pYLEX1-LIP	P_{hp4d}-LIP-T_{XPR2}, LEU2	This study
pYLEX1-CAD-ePTS1-LIP	P_{hp4d}-CAD-ePTS1-T_{XPR2}, P_{hp4d}-LIP-T_{XPR2}, LEU2	This study
pYLEX1-POX1	P_{hp4d}-POX1-T_{XPR2}, LEU2	This study
pYLEX1-CAD-ePTS1-POX1	P_{hp4d}-CAD-ePTS1-T_{XPR2}, P_{hp4d}-POX1-T_{XPR2}, LEU2	This study
pYLEX1-POX2	P_{hp4d}-POX2-T_{XPR2}, LEU2	This study
pYLEX1-CAD-ePTS1-POX2	P_{hp4d}-CAD-ePTS1-T_{XPR2}, P_{hp4d}-POX2-T_{XPR2}, LEU2	This study
pYLEX1-POX3	P_{hp4d}-POX3-T_{XPR2}, LEU2	This study
pYLEX1-CAD-ePTS1-POX3	P_{hp4d}-CAD-ePTS1-T_{XPR2}, P_{hp4d}-POX3-T_{XPR2}, LEU2	This study
pYLEX1-POX4	P_{hp4d}-POX4-T_{XPR2}, LEU2	This study
pYLEX1-CAD-ePTS1-POX4	P_{hp4d}-CAD-ePTS1-T_{XPR2}, P_{hp4d}-POX4-T_{XPR2}, LEU2	This study
pYLEX1-POX5	P_{hp4d}-POX5-T_{XPR2}, LEU2	This study
pYLEX1-CAD-ePTS1-POX5	P_{hp4d}-CAD-ePTS1-T_{XPR2}, P_{hp4d}-POX5-T_{XPR2}, LEU2	This study
pYLEX1-POX5	P_{hp4d}-POX6-T_{XPR2}, LEU2	This study
pYLEX1-CAD-ePTS1-POX6	P_{hp4d}-CAD-ePTS1-T_{XPR2}, P_{hp4d}-POX6-T_{XPR2}, LEU2	This study

pYLEX1-MFE1	P_{hp4d}-MFE1-T_{XPR2}, LEU2	This study
pYLEX1-CAD-ePTS1-MFE1	P_{hp4d}-CAD-ePTS1-T_{XPR2}, P_{hp4d}-MFE1-T_{XPR2}, LEU2	This study
pYLEX1-POT1	P_{hp4d}-POT1-T_{XPR2}, LEU2	This study
pYLEX1-CAD-ePTS1-POT1	P_{hp4d}-CAD-ePTS1-T_{XPR2}, P_{hp4d}-POT1-T_{XPR2}, LEU2	This study
pYLEX1-PEX10	P_{hp4d}-PEX10-T_{XPR2}, LEU2	This study
pYLEX1-CAD-ePTS1-PEX10	P_{hp4d}-CAD-ePTS1-T_{XPR2}, P_{hp4d}-PEX10-T_{XPR2}, LEU2	This study
Strains	**Genotype**	**Reference**
Po1g KU70Δ	MatA, leu2-270, ura3-302::URA3, xpr2-332, axp-2, ku70-	Li jian
Po1g-CAD	MatA, leu2-270, ura3-302::URA3, xpr2-332, axp-2, ku70-, CAD	This study
Po1g-hrGFP0-ePTS1	MatA, leu2-270, ura3-302::URA3, xpr2-332, axp-2, ku70-, hrGFP0-ePTS1	This study
Po1g-CAD-ePTS1	MatA, leu2-270, ura3-302::URA3, xpr2-332, axp-2, ku70-, CAD-ePTS1	This study
Po1g-CAD-ePTS1-LIP	MatA, leu2-270, ura3-302::URA3, xpr2-332, axp-2, ku70-, CAD-ePTS1-LIP	This study
Po1g-CAD-ePTS1-POX1	MatA, leu2-270, ura3-302::URA3, xpr2-332, axp-2, ku70-, CAD-ePTS1-POX1	This study
Po1g-CAD-ePTS1-POX2	MatA, leu2-270, ura3-302::URA3, xpr2-332, axp-2, ku70-, CAD-ePTS1-POX2	This study
Po1g-CAD-ePTS1-POX3	MatA, leu2-270, ura3-302::URA3, xpr2-332, axp-2, ku70-, CAD-ePTS1-POX3	This study
Po1g-CAD-ePTS1-POX4	MatA, leu2-270, ura3-302::URA3, xpr2-332, axp-2, ku70-, CAD-ePTS1-POX4	This study
Po1g-CAD-ePTS1-POX5	MatA, leu2-270, ura3-302::URA3, xpr2-332, axp-2, ku70-, CAD-ePTS1-POX5	This study
Po1g-CAD-ePTS1-POX6	MatA, leu2-270, ura3-302::URA3, xpr2-332, axp-2, ku70-, CAD-ePTS1-POX6	This study

Po1g-CAD-ePTS1-MFE1	MatA, leu2-270, ura3-302::URA3, xpr2-332, axp-2, ku70-, CAD-ePTS1-MFE1	This study
Po1g-CAD-ePTS1-POT1	MatA, leu2-270, ura3-302::URA3, xpr2-332, axp-2, ku70-, CAD-ePTS1-POT1	This study
Po1g-CAD-ePTS1-PEX10	MatA, leu2-270, ura3-302::URA3, xpr2-332, axp-2, ku70-, CAD-ePTS1-PEX10	This study
Po1g-CAD-ePTS1-ICLΔ	MatA, leu2-270, ura3-302::URA3, xpr2-332, axp-2, ku70-, CAD-ePTS1-ICLΔ-hph	This study
Po1g-CAD-ePTS1-ICLΔ	MatA, leu2-270, ura3-302::URA3, xpr2-332, axp-2, ku70-, CAD-ePTS1-CATΔ-hph	This study

Table S2. Primers used in PCR

DNA targets	Primer	Sequence
CAD	CAD1-F	acaaccacacacatccacaATGACCAAACAATCTGCGGACA
CAD	CAD1-R	TGCTGCAACAGGCCCCAGTTTCTGTCCATATCCAATCACCCTGC
CAD	CAD2-F	GCAGGGTGATTGGATATGGACAGAAACTGGGGCCTGTTGCAGCA
CAD	CAD2-R	ttagtttcgggttcccacgtgTTATACCAGTGGCGATTTCACG
hrGFPO-ePTS1	GFP-ePTS1-F	acaaccacacacatccacAATGGTGTCTAAGCAGATCCTGAAGA
hrGFPO-ePTS1	GFP-ePTS1-R	ttagtttcgggttcccagcttggatcgtcgtcctcggcccagcacgtgGTGGTGGTGGTGGTGGTGC
CAD-ePTS1	CAD-ePTS1-R	ttagtttcgggttcccacgtgTTAcagcttggatcgtcgtcctcggcccagTACCAGTGGCGATTTCACG
LIP	LIP-F	acaaccacacacatccacaATGGTCAGCTTTGGAGCTCG
LIP	LIP-R	ttagtttcgggttcccacgtgTTAGTTGGAGAGCTCGAGACCC
POX1	POX1-F	acaaccacacacatccacAATGGCCAAGGAGCGAGGT
POX1	POX1-R	ttagtttcgggttcccacgtgTCACTCATCGAGATCGCAAATTT
POX2	POX2-F	acaaccacacacatccacAATGAACCCCAACAACACTGGC
POX2	POX2-R	ttagtttcgggttcccacgtgCTATTCCTCATCAAGCTCGCAA
POX3	POX3-F	acaaccacacacatccacAATGATCTCCCCCAACCTCACA
POX3	POX3-R	ttagtttcgggttcccacgtgCTATTCCTCGTCCAGCTCGCA
POX4	POX4-F	acaaccacacacatccacAATGATCACCCCAAACCCCG
POX4	POX4-R	ttagtttcgggttcccacgtgTTACTGAATATCCTCGGGCTCC
POX5	POX5-F	acaaccacacacatccacAATGAACAACAACCCCACCAACG
POX5	POX5-R	ttagtttcgggttcccacgtgCTACTCGTCCAGGTCGCAAATC
POX6	POX6-F	actttggtctactccggtacAATGCTCTCTCAACAGTCCCTCAA
POX6	POX6-R	gggacaggccatggaggtaccCTACTCATCCTCAAGAGAGCAAATTT
MFE1	MFE1-F	actttggtctactccggtacAATGTCTGGAGAACTAAGATACGACGG

MFE1	MFE1-R	gggacaggccatggaggtaccTTAGAGCTTAGCATCCTTGGGG
POT1	POT1-F	acaaccacacacatccacAATGGACCGACTTAACAACCTCG
POT1	POT1-R	ttagtttcgggttcccacgtgTTACTCGGCAACAACCAGAGAA
PEX10	PEX10-F	actttggtctactccggtacAATGGACTACTTTTCGTCACTCAACG
PEX10	PEX10-R	gggacaggccatggaggtaccTTACACCATCAGTCGTCTCAGACC
Co-overexpression (general primer)		
-	CAD-ePTS1-LIP-F	ccatccagcctcgcgtcgcCCCGCGCCCACCGGAAG
-	CAD-ePTS1-LIP-R	acgtcttgctggcgttcgcgaCATGAGAATTCGGACACGGG
Gene knockout		
ICL-less	ICL-up-F	ccttttgccagtatatcca
ICL-less	ICL-up-R	agggtattctgggcctccatgtcttttgtatgcttggtcagtcta
ICL-less	ICL-down-F	atgtgaatgctggtcgctatactggcagtttgtttagcaaaatatatt
ICL-less	ICL-down-R	agtaggttgtctggcttttcct
ICL-hph	ICL-hph-F	tagactgaccaagcatacaaaagacatggaggcccagaataccct
ICL-hph	ICL-hph-R	aatatattttgctaaacaaactgccagtatagcgaccagcattcacat
CAT-less	CAT-up-F	atataccgaggcatgcaatttgat
CAT-less	CAT-up-R	caaggagggtattctgggcctccatgtcggtgaaagcgcgggtagacgtgagtcgagc
CAT-less	CAT-down-F	gtatgtgaatgctggtcgctatactgatgcggttaaaagttcaagtaaaataatgat
CAT-less	CAT-down-R	gacgagcatctcgaatcgaag
CAT-hph	CAT-hph-F	gctcgactcacgtctacccgcgctttcaccgacatggaggcccagaataccctccttg
CAT-hph	CAT-hph-R	atcattattttacttgaacttttaaccgcatcagtatagcgaccagcattcacatac

SUPPLEMENTARY FIGURES

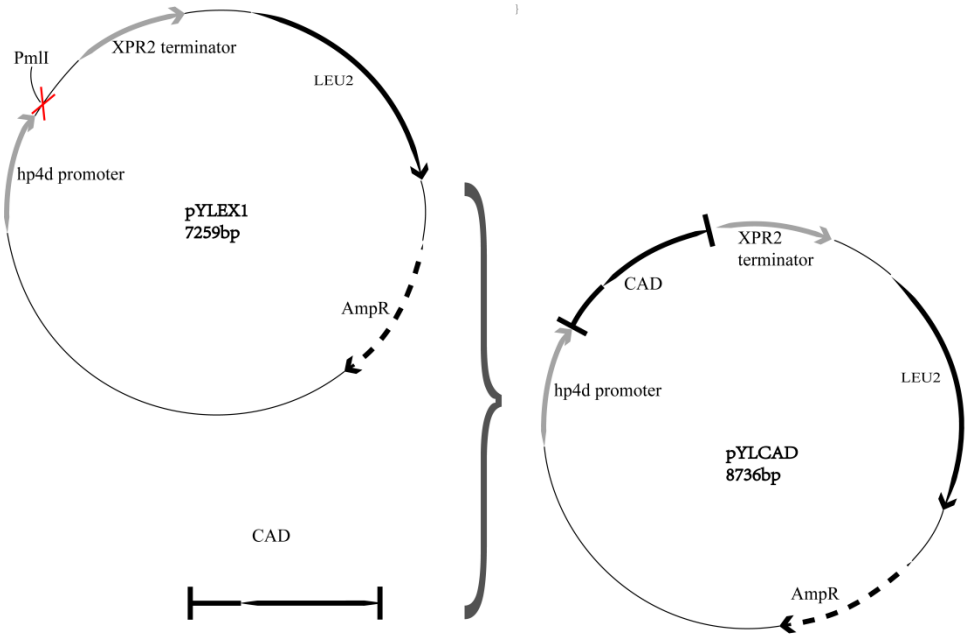

Figure S1. Assembly of plasmid pYLEX1-CAD. CAD gene isolated from *A. terraeus* was cloned into the Pml I site of pYLEX1 with a primer pair CAD1-F/CAD2-R to generate plasmid pYLEX1-CAD.

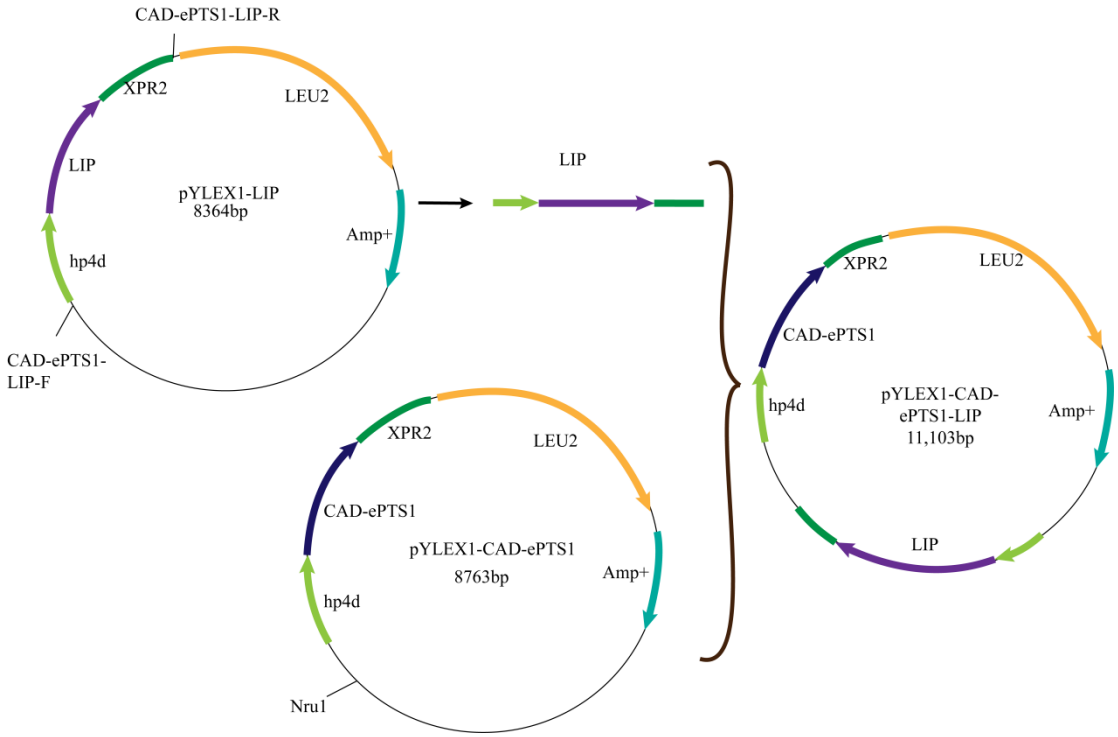

Figure S2. Assembly of plasmid pYLEX1-CAD-ePTS1-LIP. The expression cassette of LIP was cloned into pYLEX1-CAD-ePTS1 with primers CAD-ePTS1-LIP-F/R to generate plasmid pYLEX1-CAD-ePTS1-LIP.

REFERENCES

Li, J., Zhu, K., Miao, L., Rong, L. X., Zhao, Y., Li, S. L., et al. (2021). Simultaneous Improvement of Limonene Production and Tolerance in Yarrowia lipolytica through Tolerance Engineering and Evolutionary Engineering. ACS. Synth. Biol. 10, 884-896. doi: 10.1021/acssynbio.1c00052